Efficiency of ZnO Nanoparticles in the Treatment of Effluent Contaminated with Remazol Yellow Gold

Eficiência das Nanopartículas de ZnO no Tratamento de Efluente Contendo Amarelo Ouro Remazol

Guilherme Leocardio Lucena[1], Renata Júlia Cordeiro Araújo[2], Rafael Pereira da Silva[3], Anely Maciel de Melo[4] and Max Rocha Quirino[5]

ABSTRACT

Zinc oxide (ZnO) was synthesized by the short-time microwave-assisted hydrothermal method and characterized by X-Ray Diffraction, Scanning Electron Microscopy and N_2 adsorption-desorption techniques. The photocatalytic activity of ZnO was evaluated on the basis of the degradation of gold yellow remazol azo dye (RNL) in the presence of UVC irradiation. The effects of dye concentration, photocatalyst mass, and pH of the dye solution was investigated. The characterizations of the material showed the formation of a hexagonal phase with a high long-range order and the formation of particle aggregates, resulting in a quasi-spherical morphology. Photocatalysis experiments showed a high photocatalytic efficiency (92 %) in dye degradation over a short period of time. Under acidic conditions and low dye concentrations, the photocatalytic effect was more effective. RNL photodegradation followed the pseudo-first-order kinetic model. The Langmuir-Hinshelwood (L-H) model was used to describe the photocatalytic process.

keywords   zinc oxide, photocatalytic degradation, hydrothermal method, azo dye

RESUMO

Óxido de Zinco (ZnO) foi sintetizado em curto tempo pelo método hidrotermal assistido por micro-ondas e caracterizado pelas técnicas de Difração de Raios-X, Microscopia Eletrônica de Varredura e adsorção-dessorção de N_2. A atividade fotocatalítica do ZnO foi avaliada na degradação do azo corante amarelo ouro remazol (RNL) na presença de irradiação UVC. O efeito da concentração do corante, massa do fotocatalisador e pH da solução do corante foi investigado. As caracterizações mostraram a formação de ZnO fase hexagonal com alta ordem a longo alcance e formação de agregados particulados resultando em uma morfologia quase esférica. Os ensaios de fotocatálise mostraram alta eficiência fotocatalítica (92 %) na degradação do corante, em curto espaço de tempo. Em condições ácidas e baixas concentrações de corante, o efeito fotocatalítico foi mais eficaz. A fotodegradação RNL seguiu o modelo cinético de pseudo-primeira ordem. O modelo Langmuir-Hinshelwood (L-H) foi usado para descrever o processo fotocatalítico.

palavras-chave   óxido de zinco, degradação fotocatalítica, método hidrotermal, azo corante

[1]Dr., Dept. of Basic, Social and Agricultural Sciences, UFPB, Bananeiras, PB, Brazil. guilhermelucena@cchsa.ufpb.br
[2]Graduation Student, Agroindustry, UFPB, Bananeiras, PB, Brazil. renatajulia1998@gmail.com
[3]Graduation Student, Agroindustry, UFPB, Bananeiras, PB, Brazil. rafaelps19972015@gmail.com
[4]Dr. Prof., Dept. of Agro. Mgmt. and Tech., UFPB, Bananeiras, PB, Brazil. anely-maciel@live.com
[5]Dr. Prof., Dept. of Basic, Social and Agricultural Sciences, UFPB, Bananeiras, PB, Brazil. maxrochaq@gmail.com

Semin., Ciênc. Exatas Tecnol. 2024, v.45: e49498

1

Introduction

Azo dyes are organic compounds with chemically complex structures represented by the $R - N = N - R'$ bond (chromophore group), where R and R' can be aryl or alkyl compounds. Such compounds are widely used in the textile, paper and food industries (Alsantali et al., 2022; Benkhaya et al., 2020; Vaiano & De Marco, 2023). This class of dyes pollutes the aquatic environment, reducing light penetration and solubility, interfering the photosynthetic potential of phytoplankton, altering the pH, increasing biochemical and chemical oxygen demands (Alzain et al., 2023).

Due to good stability under environmental conditions, effluents containing azo dyes can cause serious environmental problems. Because, when dumped into lakes, rivers or groundwater, they favor the contamination of bodies of water, causing health risks due to their lethal effect, genotoxicity, mutagenicity and carcinogenicity (Chung, 2016). A study indicated that 98% of organic azo dyes were lethal to fish (LC50) at a concentration greater than 1 mg.L^{-1} (Carmen & Daniela, 2012).

The azo dyes toxicity is due to the formation of aromatic amines or the benzidine molecule under reductive conditions. After toxic aromatic amine intermediates released into water through reduction, they can damage vital organs such as the liver, kidney, central nervous system, and reproductive system in humans and prevent photosynthesis in plants (Uday et al., 2016; Weldegebrieal, 2020). Some studies indicate that benzidine has a direct relationship with human bladder cancer. Additionally, there is a higher incidence of bladder cancer in dyers exposed to azo dyes (Puvaneswari et al., 2006).

In this context, Advanced Oxidative Processes (AOPs) have received special attention in the treatment of effluents containing organic dyes, as they have proven to be efficient in the treatment, since, by producing free radicals, they cause chain reactions, therefore making the treatment effective of decontamination process (Vaiano & De Marco, 2023; Yassumoto et al., 2009). Among AOPs, heterogeneous photocatalysis using semiconductors has been widely investigated and has shown good results, as it favors the mineralization of organic dyes into H_2O, CO_2 and mineral acids, without causing secondary pollution (Chen et al., 2017).

Zinc oxide (ZnO) is one of the most used semiconductors in heterogeneous photocatalysis processes due to its high redox potential, low cost, non-toxicity and for being an ecological catalyst due to its harmless nature (Manikanika & Chopra, 2022). Some studies report that ZnO exhibits greater efficiency in the photocatalytic degradation of some organic dyes than TiO_2 (Ansari et al., 2013; Lee et al., 2015).

Several methods have been used for the synthesis of ZnO nanostructures such as solid state reaction, chemical precipitation, sol-gel, ultrasonic solvothermal (Surbhi et al., 2023; Weldegebrieal, 2020). However, the hydrothermal method is the most promising due to its simplicity and low cost. However, several syntheses based on this method took several hours to complete. The introduction of microwave irradiation in the hydrothermal method promotes an increase in crystallization kinetics by one or more orders of magnitude, resulting in shorter reaction times (Komarneni et al., 1992; Schimidt et al., 2022; Sun et al., 2016).

Hasanpoor et al. (2015) synthesized ZnO nanoparticles using the microwave-assisted hydrothermal method. The authors found that changes in microwave power and irradiation time promoted changes in the morphology of the material. Alfarisa et al. (2019), using the same synthesis method, synthesized ZnO micro-nanostructures in a fast time. According to the authors, the rapid heating process generated from the rotation, friction and collisions of water molecules inside the microwave resulted in a faster reaction process compared to the conventional hydrothermal method.

This work presents the rapid ZnO synthesis nanoparticles by the microwave-assisted hydrothermal method and its application as a photocatalyst for the degradation of the azo organic dye yellow gold remazol (RNL). A study of the reaction kinetics correlating the reaction conditions, mechanism and properties of the photocatalyst was evidenced.

Materials and methods

Synthesis of ZnO nanoparticles

Zinc oxide (ZnO) nanoparticles were synthesized by the microwave-assisted hydrothermal method as described by Quirino et al. (2017). In the present work, a zinc nitrate solution was prepared, ($Zn(NO_3)_2$.6H_2O, 98 %, SIGMA-ALDRICH) with a concentration of 9 mmol.L^{-1}. In 132 mL of this solution, 8 mL of a

2

Semin., Ciênc. Exatas Tecnol. 2024, v.45: e49498

sodium hydroxide solution (NaOH, 98 %, VETEC), with 5 mol.L^{-1} concentration, and 3.6 g of polyethylene glycol (PEG 400, U.S.P., SYNTH) were added.

The precursor solution was transferred to a sealed Teflon autoclave and placed in a microwave reactor, undergoing microwave-assisted hydrothermal treatment ($f = 2450$ MHz, maximum power = 800 W). The synthesis was carried out at 100 ºC for 5 min and heating rate of 20 ºC.min^{-1}. After hydrothermal treatment, a white precipitate formed, which was washed repeatedly with distilled water until neutral pH. Subsequently, the material was filtered and transferred to an oven for drying at 110 ºC for 12 h. The sample was named ZONa05P.

Characterization

The synthesized material was characterized by X-ray diffraction (XRD) techniques using a diffractometer (XRD-6000, Shimadzu) operating at 40 kV and 40 mA with CuKα radiation. The diffractograms were collected in the range of $15º - 80º$ (2θ), using a step of 0.02º and a step time of 2 s. The average crystallite size (ε) was determined by the Debye-Scherrer equation, as described in equation (1),

$$\varepsilon = \frac{K\lambda}{\beta \cos \theta},$$

(1)

where K is form factor; λ is the wavelength; β is the peak width at half height; θ is the Bragg diffraction angle.

The agglomerates morphology of the obtained sample was observed using a scanning electron microscope, SEM (Philips, XL30). The textural characteristics of the sample (surface area, pore size and pore volume) were determined by the nitrogen adsorption and desorption technique using the BET (Brunauer, Emmett and Teller) and BJH (Barret, Joyner and Halenda) methods in a ASAP 2000 Micromeritics device.

Photocatalytc tests

The sample ZONa05P was evaluated as a photocatalyst in the degradation of the azo dye Remazol Yellow Gold (RNL), from Dystar. The dye has the molecular formula $CH_{16}N_4O_{10}S_3Na_2$, molar weight 566.49 g.mol^{-1} and 1 azo bond in its structure, Figure 1.

Figure 1 - Remazol Yellow Gold Chemical structure.
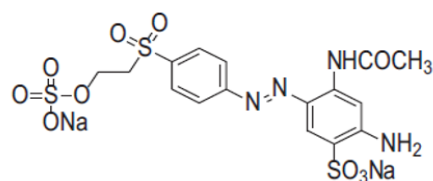
In order to understand how to reduce the action of possible interferers in the photocatalysis process, it was decided to prepare aqueous solutions of the azo dye RNL in order to simulate possible effluents. In this way, stock solutions were prepared with concentrations of 0.01 mmol.L^{-1}, 0.03 mmol.L^{-1}, 0.05 mmol.L^{-1}, 0.07 mmol.L^{-1} and 0.09 mmol.L^{-1}. pH adjustments (2, 4, 6, 8 and 10) were carried out using HCl and NaOH solutions both at 0.1 mol.L^{-1}.

The photocatalytic tests were carried out in a rectangular wooden reactor, with dimensions of 10 cm $\times$ 20 cm $\times$ 100 cm, using a UVC lamp (λ = 254 nm, ILUMISAMPA). The experiments were tested in Petri dishes, in triplicates, using masses of 5 mg, 10 mg, 15 mg and 20 mg of the photocatalyst (ZONa05P) and 10 mL of the RNL dye solution at different initial concentrations. The mixtures were photoirradiated for a period of 10 to 80 min. After photocatalysis, the samples were centrifuged and filtered as shown in Figure 2. The percentage of decolorization and degradation of the dye solutions was quantified using a UV-vis spectrophotometer (UV-2550, Shimadzu) by measuring the absorbance of the RNL solution in 411 nm, which is directly associated with the chromophoric group ($-N = N-$) (Catanho et al., 2006).

Semin., Ciênc. Exatas Tecnol. 2024, v.45: e49498

3

The removal rate (R %) of the azo dye was calculated by equation (2):

$$\text{R\%} = \frac{C_0 - C_t}{C_0} \cdot 100 \text{ \%},\tag{2}$$

where C_0 and C_t are the concentrations of the azo dye before photocatalysis and at different irradiation times, respectively.

**Figure 2 -** Scheme of photocatalysis tests.
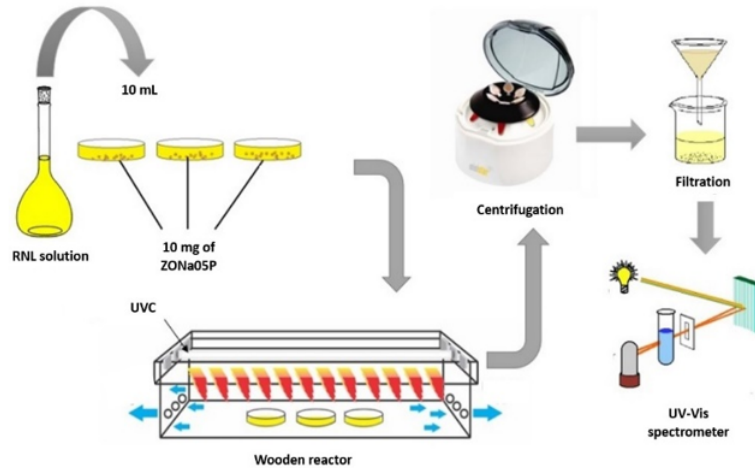
Results and Discussions

Characterization of ZnO nanoparticles

Figure 3 presents the results of the characterization of ZONa05P synthesized in a short time by the microwave-assisted hydrothermal method.

Figure 3 - haracterization of ZONa05P synthesized via the microwave-assisted hydrothermal method: (a) XRD and (b) SEM at 5×10^3x magnification.

(a) (b)
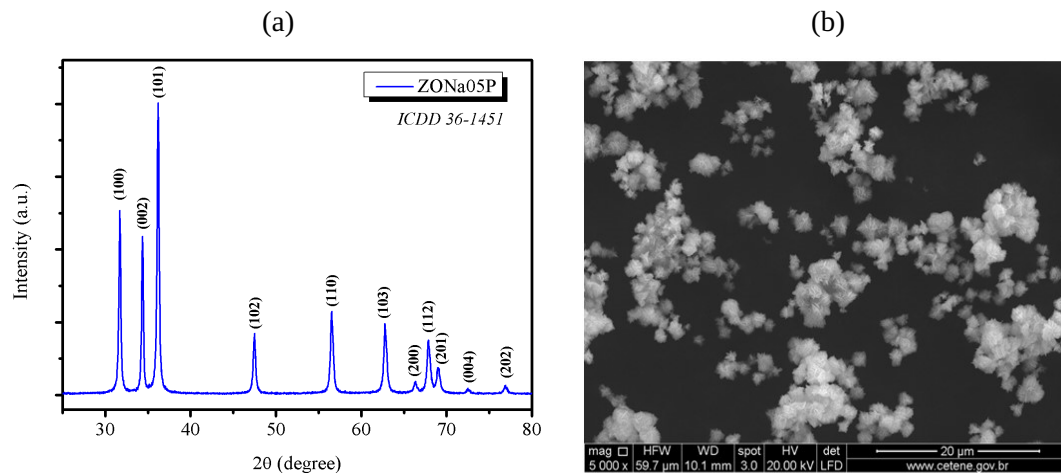
In Figure 3(a), the X-ray diffractogram showed the formation of ZnO with hexagonal phase (space group P63mc) with peaks consistent with the ICCD $36 - 1451$ pattern. Furthermore, long-range secondary phase formation was not observed. Lattice parameters were calculated using the Rede93 software developed by UNESP, Araraquara, Brazil. These parameters for the ZONa05P sample were $a = 3.251$ and $c = 5.207$. These values are consistent with the reference parameter values $a = 3.249$ and $c = 5.206$ shown on the ICDD card.

Chankhanittha and Nanan (2018) synthesized ZnO by the conventional hydrothermal method (without microwave irradiation) using NaOH as a mineralizing agent and obtained a material with long-range crystallite size (D_{XRD}) ranging from $46 - 51$ nm. It is worth noting that they did not use PEG and that the synthesis time was 24 h. In the present work, the synthesis of ZnO occurred in just 5 minutes with a crystallite size of 34.9 nm. These data indicate that the introduction of PEG and irradiation by microwave waves enabled the formation of a material with high crystallinity, of nanometric order, in a short synthesis time. Analysis of the SEM image, as depicted in Figure 3(b), showed that ZONa05P presented lamellar clusters, resulting in an almost spherical shape, with dimensions less than 5 μm.

Figure 4 shows the nitrogen adsorption-desorption isotherms of the ZONa05P sample.

Figure 4 - Characterization of ZONa05P synthesized via the microwave-assisted hydrothermal method: (a) Isotherm of adsorption and desorption of N_2 and (b) pore size distribution.
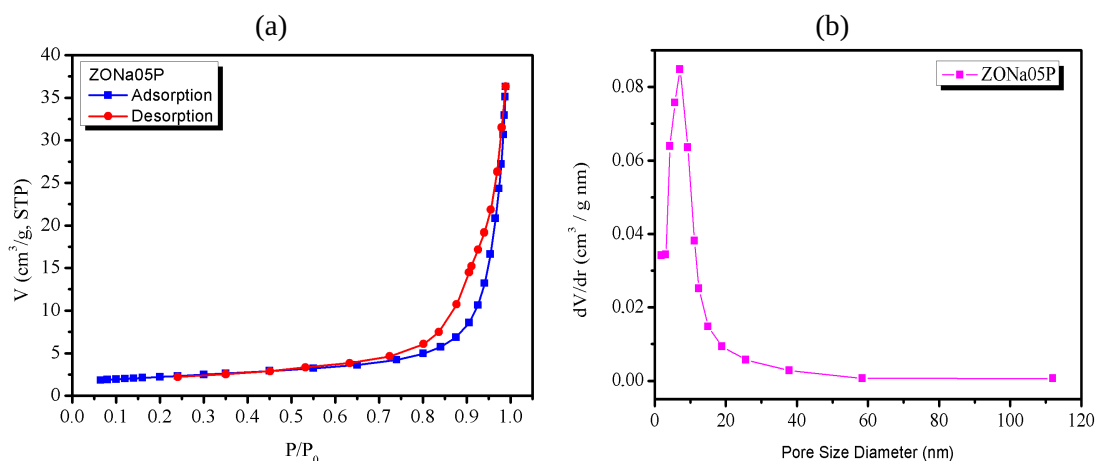

The N_2 adsorption and desorption isotherms, shown in Figure 4(a), indicated that the material ZONa05P is of the H-3 loop type, according to the IUPAC classification (Sing et al., 1985), which is typical of N_2 aggregates with slit pores. The data showed that the material has a specific surface area of $7.64 m^2.g^{-1}$. Regarding the pore size distribution (BJH method applied to the desorption isotherm), Figure 4(b), the average pore size was observed to be around 15 nm, although the largest pore population varied from 7 to 15 nm.

Photodegradation of RNL and the effect of the initial concentration (C_0)

The effect of the initial concentration (C_0) study of the azo dye on photocatalytic degradation was carried out by varying the concentration of the RNL solution from 0.01 to 0.09 mmol.L^{-1}). In this study, the mass of ZONa05P was set at 10 mg, pH 6.0, solution volume of 10 mL and irradiation time of 80 min. Removal rates (R %) are shown in Figure 5.

Figure 5 - Removal rate (R %) by ZONa05P at different C_0 values of the azo dye RNL, at pH 6.0 and contact time of 80 min.


Semin., Ciênc. Exatas Tecnol. 2024, v.45: e49498

5
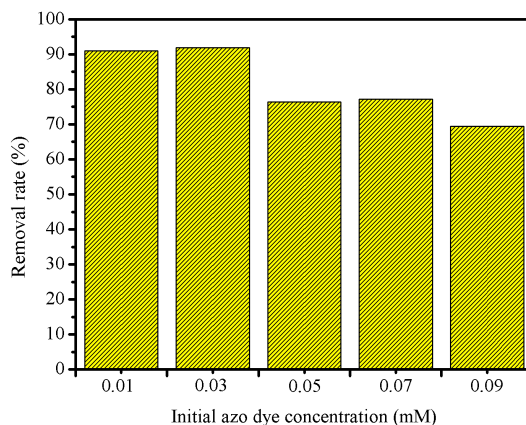
The data showed that at low concentrations (0.01 mmol.L^{-1} and 0.03 mmol.L^{-1}) the highest removal rate occurred, $91\,\%$ and $92\,\%$, respectively. As the concentration of the azo dye increases, there is a tendency for the R % to decrease. Similar results were observed by Kaur et al. (2013) at the photodegradation of methyl orange azo dye by ZnO particles. This phenomenon may occur due to saturation of the photocatalyst, since a greater quantity of azo dye molecules adsorb at the surface competing for the material active sites. Furthermore, as the removal rate is associated with the number of electron/hole pairs (e$^-$/h$^+$) photogenerated, considering that the mass of the photocatalyst remained constant and that amount of hydroxyl radicals generated did not increase either, it was expected that the removal rate decreased with increasing azo dye concentration. Based on these results, it was decided to continue the study by setting the initial concentration of the RNL dye at 0.03 mmol.L^{-1}.

Effect of UVC radiation on the photocatalytic degradation of RNL

In order to understand the action of UVC lamp radiation on the dye photodegradation process, the initial conditions of RNL solution (0.03 mmol.L^{-1}), pH= 6.0 and the mass of ZONa05P (10 mg). A sample of the dye solution without addition of ZONa05P was also submitted to radiation to evaluate the natural photolysis process. The UVC photoirradiation time totaled 80 min. In contrast, a sample was subjected to contact with ZnO nanoparticles in the absence of UVC irradiation (dark with ZONa05P) for 80 min.

Figure 6 shows the R % of the RNL dye due to photolysis in the presence and absence of ZONa05P and in the dark.

Figure 6 - Removal rate (R %) by photolysis in the presence and absence of ZONa05P and in the dark with ZONa05P, after 80 min, at pH 6.0.
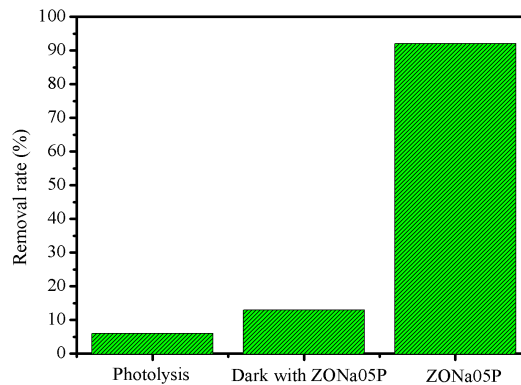
When evaluating the degradation of the dye in the absence of the catalyst (photolysis without ZONa05P) and with the catalyst in the absence of ultraviolet light (dark with ZONa05P), the percentages of degradation, for the same reaction time, were $6\,\%$ and $13\,\%$, respectively. These results indicate that the removal process is favored (92 %) only when was submitted to irradiation.
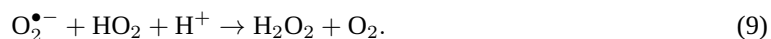
This effect is only reached because, when ZONa05P is irradiated with a light source ($h\upsilon$) whose energy is equal to or greater than the band gap of the material, the electron (e$^-$) is promoted from the valence band (BV) to the conduction band (BC), resulting in the formation of e$^-$/h$^+$ pairs as shown in equation (3):

$$ZONa05P + h\upsilon \rightarrow h^+ + e^-. \tag{3}$$

As a consequence, e$^-$/h$^+$ pairs give the semiconductor material redox properties, promoting the direct degradation of the dye molecules (Shen et al., 2015). This electron/hole pair can be rapidly recombined through surface material defects or interact with the acceptor (R) or donor molecule (D) adsorbed on the surface, as shown in equations (4) and (5):

$$R_{ads} + e^-_{BC} \rightarrow R^-_{ads}; \tag{4}$$

$$D_{ads} + h^+_{BV} \rightarrow D^+_{ads}. \tag{5}$$

Furthermore, electron/hole molecules of azo dye oxidation can occur due the formation of hydroxyl (•OH) or superoxide ($O_2^{\bullet-}$) radicals. This last chemical species (superoxide) can form peroxides (H_2O_2) as shown in equations (6) to (9):

$$H_2O + h^+ \rightarrow H^+ + \bullet OH; \tag{6}$$

$$OH^- + h^+ \rightarrow \bullet OH; \tag{7}$$

$$e^- + O_2^- \rightarrow O^{\bullet-}; \tag{8}$$

$$O_2^{\bullet-} + HO_2 + H^+ \rightarrow H_2O_2 + O_2. \tag{9}$$

Finally, these generated radicals react directly with the azo dye promoting the formation of inorganic compounds, CO_2 and H_2O, equation (10) (Chen et al., 2017; Shen et al., 2015).

$$O_2^{\bullet-} / \bullet OH + \text{azo dye} \rightarrow CO_2 + H_2O + \text{inorganic molecules.} \tag{10}$$
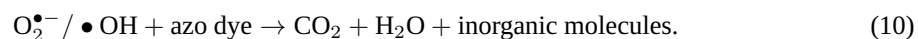
Effect of mass

The effect of photocatalyst dosage on photodegradation of azo dye RNL was evaluate by varying the mass of ZONa05P by 5 mg, 10 mg, 15 mg and 20 mg. For this study, the C_0 of the azo dye was set at 0.03 mmol.L^{-1}, solution volume of 10 mL, pH 6.0 and irradiation time of 80 min. R % are shown in Figure 7.

Figure 7 - Removal rate (R %) of the azo dye RNL by ZONa05P in different masses.
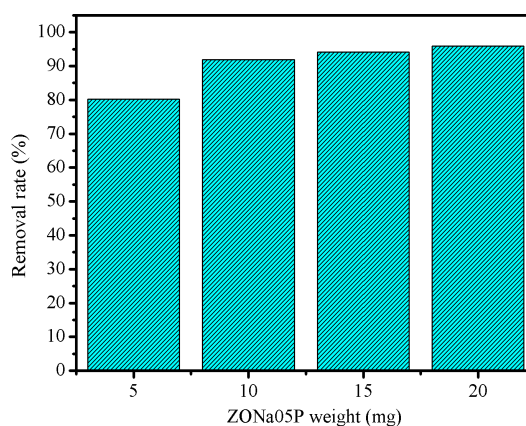
It was observed that 5 mg of ZONa05P photocatalyst promoted 80% degradation of the azo dye. When doubling the amount of ZONa05P the degradation was 92%, which corresponded to an increase of 12 percentage points. For samples containing 15 mg and 20 mg, the degradation percentages were close to 96%. When comparing the percentages of degradation between 10 mg and 20 mg, the increase was only 3 percentage points. These results indicate that, for these reaction conditions, the dosage of material greater than 10 mg does not promote significant changes in the photodegradation process. As the increase of photocatalyst amount promotes an increase in the turbidity of the solution, this provides a lower penetration of UV radiation due to increased light scattering.

Effect of pH

Figure 8 shows the R % by ZONa05P, in different initial pH conditions, and the pH value of the zero charge potential (pH_{PCZ}) of ZONa05P, obtained according to the methodology described by Robles and Regalbuto (2004). For this study, the C_0 of the azo dye was fixed at 0.03 mmol.L^{-1}, a solution volume of 10 mL, 10 mg of photocatalyst mass and an 80 min of irradiation time.

The pH of azo dye solution to be degraded through heterogeneous catalysis is a key parameter in the photocatalysis process. Typically, industrial effluents containing azo dyes have a wide pH range. In Figure 8 (a) it was observed that ZONa05P presented a percentage degradation between 77% and 93%, in the pH range evaluated. The removal rate of the azo dye RNL showed a small increase at acidic pH when compared to the

solution at natural pH (pH = 6.0). However, at alkaline pH, there is a decrease in the rate of degradation. Similar results have been reported in the literature for other azo dyes (Chen et al., 2017; Paz et al., 2014; Thomas et al., 2016). This phenomenon can be attributed to the charge density acquired on the photocatalyst surface.

Figure 8 - Effect of pH on RNL photocatalysis by ZONa05P as a function of PCZ: (a) R % for ZONa05P at different pH values and (b) ΔpH vs initial pH.
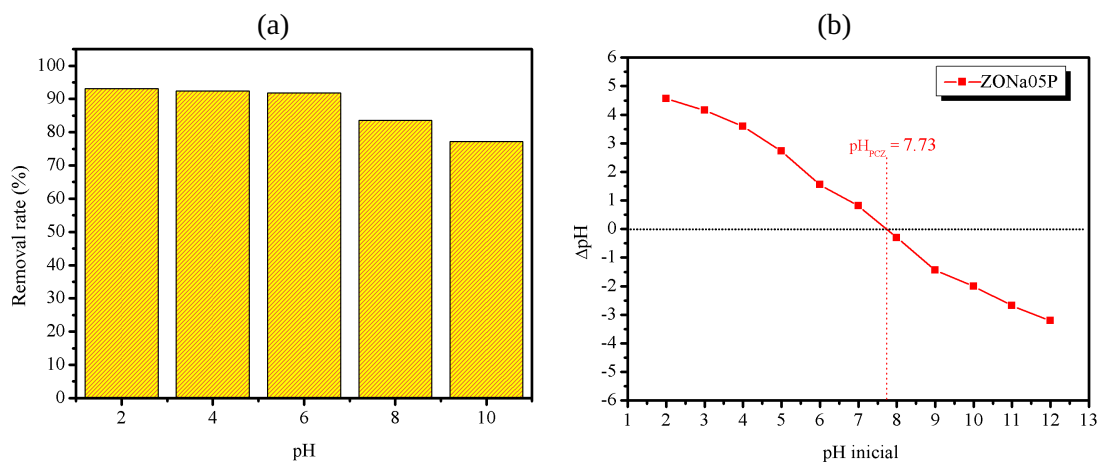
According to the graph, of initial pH vs ΔpH, shown in Figure 8(b), the point at which the ΔpH value is zero corresponds to the zero charge potential (PCZ), indicating how positive or negative the surface of the material is (Mahmood et al., 2011). Thus, it was observed that the ZONa05P sample presented $pH_{PCZ} = 7.73$. In general, when the pH solution is lower than the pH_{PCZ} value, the surface of the material acquires a positive charge density, favoring the adsorption of anions, while at a pH higher than the pH_{PCZ} the surface becomes negatively charged, thus favoring the cation adsorption (Zhu et al., 2012).

The literature indicates that the RNL dye has three pK_a values: 3, 3.5 and 6. The first value corresponds to the deprotonation of the sulfonic group, the second refers to the sulfate group and the third to the amide group (Lucena et al., 2017; Teixeira et al., 2012), whereas this complete deprotonation only occurs at pH greater than 6, leading to a greater tendency for negative charges. Thus, the forces of attraction between the ZONa05P surface charges and the negative groups of the azo dye are stronger when the pH of the solution is lower than pH_{PCZ}. This justify the photodegradation behavior with higher percentages at acidic pH, as observed in Figure 8(a). Furthermore, in acidic pH, a large O_2 amount of may have been reduced to $O^{\bullet-}$, as the positively charged surface of ZONa05P is conducive to photoelectron transfers to the photocatalyst surface (Chen et al., 2017).

Removal Kinetics

The influence of contact time on photodegradation is presented in Figure 9. The data showed that with 10 min of UVC irradiation the R % reached 55 % and that there is a tendency for growth as time increases, with the percentage maximum obtained at 80 min. Furthermore, it was noticed that between $30 - 40$ min there were no significant changes and that between $60 - 70$ min there was a small increase of 2 %.

Based on the data obtained in this study, an evaluation of the photodegradation kinetics of the azo dye RNL was carried out using the pseudo-first order linearized model, described by equation (11),

$$\ln \left(\frac{C_0}{C_f} \right) = K_{app} \cdot t, \tag{11}$$

where: K_{app} is the degradation rate constant (min^{-1}); C_0 and C_f are the initial and final concentrations of the dye (mmol.L^{-1}) before and after the photocatalysis process, respectively, and t is the irradiation time (min).

8

Semin., Ciênc. Exatas Tecnol. 2024, v.45: e49498

Figure 9 - R % for ZONa05P depending on time
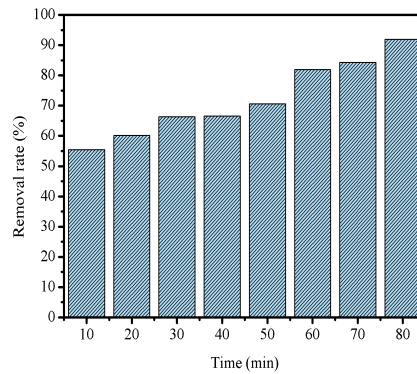
For the kinetic study, the initial concentration of the azo dye RNL varied from 0.01 mM to 0.09 mM. The results are shown in Figure 10 and the correlation coefficients (R^2) are shown in Table 1.

Figure 10 - Kinetic evaluation of RNL photocatalysis by ZONa05P: (a) Pseudo-first order kinetic curve and (b) Graph of $1/K_{app}$ *vs* C_0 of the azo dye RNL.
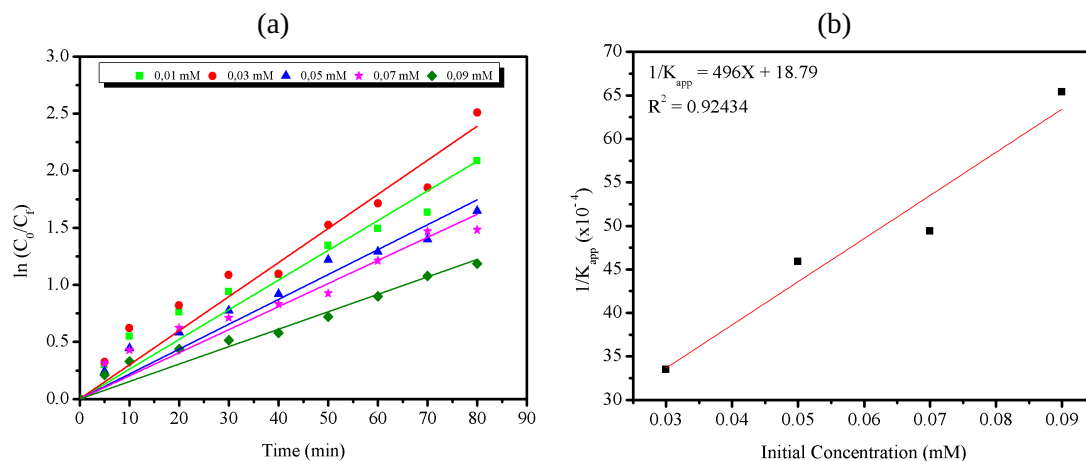
Table 1 - Pseudo-first order kinetic constants and correlation coefficients for degradation of the azo dye RNL after photocatalysis.

C_0 (mmol.L^{-1})	R %	K_{app} (min^{-1})	R^2
0.01	91	2.604×10^2	0.98108
0.03	92	2.987×10^2	0.98152
0.05	76	2.180×10^2	0.98313
0.07	77	2.023×10^2	0.97617
0.09	70	1.528×10^2	0.98283

Considering the equations of the straight lines obtained from Figure 10(a), the values of the correlation coefficients (R^2) indicated that the photodegradation of the azo dye fits the pseudo-first order kinetic model. Among all the concentrations tested, $C_0 = 0.03$ mmol.L^{-1} was the one with the highest K_{app} value (2.987×10^{-2}). Furthermore, it was observed that as the dye concentration increased, the degradation rate constant decreased, except the concentration range $0.01 - 0.03$ mmol.L^{-1}. Similar results were reported by Kaur et al. (2013) when evaluating the photodegradation of methyl orange azo dye by ZnO particles synthesized by the oxalate precursor thermal decomposition method.

To describe the photocatalysis processes of organic dyes in aqueous solutions, several researchers have used the Langmuir-Hinshelwood (L-H) kinetic model to explain the solid-liquid interface processes (Barka et al.,

Semin., Ciênc. Exatas Tecnol. 2024, v.45: e49498

9

2010; Ertugay & Acar, 2017) according to equation (12),

$$\frac{1}{K_{\text{app}}} = \frac{1}{K_1 K_2} + \frac{C_0}{K_1},$$ (12)

where: K_{app} is the degradation rate constant (min^{-1}); K_1(mol.L^{-1}.min^{-1}) is the surface reaction rate constant; K_2(L.mol^{-1}) is the Langmuir-Hinshelwood adsorption equilibrium constant and C_0 is the initial concentration (mol.L^{-1}) of the azo dye.

The L-H mechanism postulates that the solid-catalyzed reaction in the liquid phase occurs between species adsorbed on the material surface active sites. Thus, the photocatalyst increases the reaction rate through the ability to adsorb reactants so that the activation energy is significantly reduced relative to the same reaction without the photocatalyst (Hougen & Watson, 1943).

According to the data presented in Figure 10(b) and Table 1, a linear relationship between the data ($R^2 = 0.92527$) was verified, indicating that the photodegradation process of the azo dye RNL by ZONa05P can be validated by the model L-H. The values of K_1 and K_2 were calculated using the straight line equation (12) and the values obtained were 2.01×10^{-6} mol.L^{-1}.min^{-1} and 2.66×10^4 L.mol^{-1}, respectively.

Conclusions

XRD patterns and SEM image results showed that ZnO synthesis resulted in the formation of a hexagonal structure with an almost spherical morphology. The catalyst dimensions were below 5 μm and an average crystallite size of 34.9 nm. ZONa05P showed high photocatalytic efficiency in the azo dye RNL degradation with UV radiation, reaching 92 % discoloration after 80 min of reaction. The pseudo-first order kinetic model and the mechanism proposed by the Langmuir-Hinshelwood (L $-$ H) model fit for this the degradation data. The acidic condition is more favorable to photodegradation than the alkaline condition. The azo dye removal rate decreases with increasing initial dye solution concentration and increases slightly with increasing photocatalyst mass.

Author contributions

G.L. Lucena participated in conceptualization, formal analysis, investigation, visualization and writing – original draft, review and editing. R.J.C. Araújo participated in conceptualization, formal analysis, investigation, visualization and writing – original draft; visualization, validation and writing - review and editing. R.P. Silva participated in formal analysis, investigation, visualization, validation and writing - original draft, review and editing. A.M. Melo participated in visualization, validation and writing. M.R. Quirino participated in visualization, validation and writing.

Conflicts of interest

The authors certify that there is not a commercial or associative interest that represents conflict of interest in relation to the manuscript.

References

Alfarisa, S., Toruan, P. L., Dwandaru, W. S. B., Hudha, M. N., & Sumarlan, I. (2019). Microwave-assisted hydrothermal growth of ZnO micro-nano structures. *Journal of Physics: Conference Series, 1375*, 1–6. https://doi.org/10.1088/1742-6596/1375/1/012062

10

Semin., Ciênc. Exatas Tecnol. 2024, v.45: e49498

Alsantali, R. I., Raja, Q. A., Alzahrani, A. Y. A., Sadiq, A., Naeem, N., Mughal, E. U., Al-Rooqi, M. A., Guesmi, N. E., Moussa, Z., & Ahmed, S. A. (2022). Miscellaneous azo dyes: a comprehensive review on recent advancements in biological and industrial applications. *Dyes and Pigments*, *199*, 1–47. https://doi.org/10.1016/j.dyepig.2021.110050

Alzain, H., Kalimugogo, V., Hussein, K., & Karkadan, M. (2023). A review of environmental impact of azo dyes. *International Journal of Research and Review*, *10*(6), 673–689. https://doi.org/10.52403/ijrr.20230682

Ansari, S. A., Khan, M. M., Ansari, M. O., Lee, J., & Cho, M. H. (2013). Biogenic synthesis, photocatalytic, and photoelectrochemical performance of Ag-ZnO nanocomposite. *The Journal of Physical Chemistry C*, *117*(51), 27023–27030. https://doi.org/10.1021/jp410063p

Barka, N., Qourzal, S., Assabbane, A., Nounah, A., & Ichou, Y. A. (2010). Photocatalytic degradation of an azo reactive dye, Reactive Yellow 84, in water using an industrial titanium dioxide coated media. *Arabian Journal of Chemistry*, *3*, 279–283. https://doi.org/10.1016/j.arabjc.2010.06.016

Benkhaya, S., M'rabet, S., & Harfi, A. E. (2020). Classifications, properties, recent synthesis and applications of azo dyes. *Heliyon*, *6*(1), 1–26. https://doi.org/10.1016/j.heliyon.2020.e03271

Carmen, Z., & Daniela, S. (2012). Textile organic dyes–characteristics, polluting effects and separation/elimination procedures from industrial effluents–a critical overview. In T. Puzyn & A. Mostrag (Eds.), *Organic pollutants ten years after the stockholm convention - environmental and analytical update* (pp. 55–86). IntechOpen. https://doi.org/10.5772/32373

Catanho, M., Malpass, G. R. P., & Motheo, A. J. (2006). Evaluation of electrochemical and photoelectrochemical methods for the degradation of three textile dyes. *Química Nova*, *29*, 983–989. https://doi.org/10.1590/S0100-40422006000500018

Chankhanittha, T., & Nanan, S. (2018). Hydrothermal synthesis, characterization and enhanced photocatalytic performance of ZnO toward degradation of organic azo dye. *Materials Letters*, *226*, 79–82. https://doi.org/10.1016/j.matlet.2018.05.032

Chen, X., Wu, Z., Liu, D., & Gao, Z. (2017). Preparation of ZnO photocatalyst for the efficient and rapid photocatalytic degradation of azo dyes. *Nanoscale Research Letters*, *12*, 143–152. https://doi.org/10.1186/s11671-017-1904-4

Chung, K. T. (2016). Azo dyes and human health: A review. *Journal of Environmental Science and Health C*, *34*(4), 233–261. https://doi.org/10.1080/10590501.2016.1236602

Ertugay, N., & Acar, F. N. (2017). Ultrasound and UV stimulated heterogeneous catalytic oxidation of an azo dye: A synergistic effect. *Progress in Reaction Kinetics and Mechanism*, *42*(3), 235–243. https://doi.org/10.3184/146867817X14821527549095

Hasanpoor, M., Aliofkhazraei, M., & Delavari, H. (2015). Microwave-assisted synthesis of zinc oxide nanoparticles. *Procedia Materials Science*, *11*, 320–325. https://doi.org/10.1016/j.mspro.2015.11.101

Hougen, O. A., & Watson, K. M. (1943). Solid catalysis and reaction rates. *Industrial & Engineering Chemistry Research*, *35*(5), 529–541. https://doi.org/10.1021/ie50401a005

Kaur, J., Bansal, S., & Singhal, S. (2013). Photocatalytic degradation of methyl orange using ZnO nanopowders synthesized via thermal decomposition of oxalate precursor method. *Physica B*, *416*, 33–38. https://doi.org/10.1016/j.physb.2013.02.005

Komarneni, S., Roy, R., & Li, Q. H. (1992). Microwave-hydrothermal synthesis of ceramic powders. *Materials Research Bulletin*, *27*(12), 1393–1405. https://doi.org/10.1016/0025-5408(92)90004-J

Lee, H. J., H., K. J., Park, S. S., Hong, S. S., & Lee, G. D. (2015). Degradation kinetics for photocatalytic reaction of methyl orange over Al-doped ZnO nanoparticles. *Journal of Industrial and Engineering Chemistry*, *25*, 199–206. https://doi.org/10.1016/j.jiec.2014.10.035

Lucena, G. L., Lima, L. C., Honório, L. M. C., Oliveira, A. L. M., Tranquilin, R. L., Longo, E., Souza, A. G., Maia, A. S., & Santos, I. M. G. (2017). CaSnO3 obtained by modified Pechini method applied in the photocatalytic degradation of an azo dye. *Cerâmica*, *63*, 536–541. https://doi.org/10.1590/0366-69132017633682190

Mahmood, T., Saddique, M. T., Naeem, A., Westerhoff, P., Mustafa, S., & Alum, A. (2011). Comparison of different methods for the point of zero charge determination of NiO. *Industrial & Engineering Chemistry Research*, *50*(17), 10017–10023. https://doi.org/10.1021/ie200271d

Manikanika & Chopra, L. (2022). Photocatalytic activity of zinc oxide for dye and drug degradation: A review. *Materials Today: Proceedings*, *52*, 1653–1656. https://doi.org/10.1016/j.matpr.2021.11.283

Paz, D. S., Dotto, G. L., Mazutti, M. A., & Foletto, E. L. (2014). Adsorption kinetics of direct black 38 on nitrogen-doped TiO2. *Global Nest Journal*, *16*(4), 690–698. https://doi.org/10.30955/gnj.001411

Puvaneswari, N., Muthukrishnan, J., & Gunasekkaren, P. (2006). Toxicity assessment and microbial degradation of azo dyes. *Indian Journal of Experimental Biology*, *44*(8), 618–626.

Quirino, M. R., Oliveira, M. J. C., Keyson, D., Lucena, G. L., Oliveira, J. B. L., & Gama, L. (2017). Synthesis of zinc oxide by microwave hydrothermal method for application to transesterification of soybean oil (biodiesel). *Materials Chemistry and Physics*, *185*, 24–30. https://doi.org/10.1016/j.matchemphys.2016.09.062

Robles, J. O., & Regalbuto, J. R. (2004). *The Engineering of Pt/Carbon Catalyst Preparation for application on Proton Exchange Fuel Cell Membrane (PEFCM)*. University of Illinois at Chicago. https://api.semanticscholar.org/CorpusID:46982313

Schimidt, R., Gonjal, J. P., & Morán, E. (2022). Microwaves microwave-assisted hydrothermal synthesis of nanoparticles. In B. I. Kharisov & O. V. K. U. Ortiz-Mendez (Eds.), *CRC Concise Encyclopedia of Nanotechnology* (pp. 561–570). CRC Press Taylor & Francis Group. https://doi.org/10.48550/arXiv.2203.02394

Shen, T., Wang, C., Sun, J., Jiang, C., Wang, X., & Li, X. (2015). TiO2 modified abiotic-biotic process for the degradation of azo dye methyl orange. *RSC Advances*, *5*, 58704–58712. https://doi.org/10.1039/C5RA06686G

Sing, K. S. W., Everett, D. H., Haul, R. A. W., Moscou, L., Pierotti, R. A., Rouquerol, J., & Siemieniewska, T. (1985). Reporting physisorption data for gas/solid systems with special reference to the determination of surface area and porosity. *Pure and Applied Chemistry*, *57*(4), 603–619. https://doi.org/10.1351/pac198557040603

Sun, Y., Guo, H., Zhang, W., Zhou, T., Qiu, Y., Xu, K., Zhang, B., & Yang, H. (2016). Synthesis and characterization of twinned flower–like ZnO structures grown by hydrothermal methods. *Ceramics International*, *42*(8), 9648–9652. https://doi.org/10.1016/j.ceramint.2016.03.051

Surbhi, Chakraborty, I., & Pandey, A. (2023). A review article on application of ZnO-based nanocomposite materials in environmental remediation. *Materials Today: Proceedings. In press*. https://doi.org/10.1016/j.matpr.2023.02.041

Teixeira, T. P. F., Pereira, S. I., Aquino, S. F., & Dias, A. (2012). Calcined layered double hydroxides for decolorization of azo dye solutions: Equilibrium, kinetics, and recycling studies. *Environmental Engineering Science*, *29*(7), 685–692. https://doi.org/10.1089/ees.2011.0293

Thomas, M., Naikoo, G. A., Sheikh, M. U. D., Bano, M., & Khan, F. (2016). Effective photocatalytic degradation of congo red dye using alginate/carboxymethyl cellulose/TiO2 nanocomposite hydrogel

under direct sunlight irradiation. *Journal of Photochemistry and Photobiology A., 327,* 33–43. https://doi.org/10.1016/j.jphotochem.2016.05.005

Uday, U. S. P., Bandyopadhyay, T. K., & Bhunia, B. (2016). Bioremediation and detoxification technology for treatment of dye(s) from textile effluent. In E. P. A. Kumbasar, & A. E. Körlü (Eds). *Textile Wastewater Treatment.* (pp. 75-92) Intechopen. https://doi.org/10.5772/62309

Vaiano, V., & De Marco, I. (2023). Removal of azo dyes from wastewater through heterogeneous photocatalysis and supercritical water oxidation. *Separations, 10*(4), 230. https://doi.org/10.3390/separations10040230

Weldegebrieal, G. K. (2020). Synthesis method, antibacterial and photocatalytic activity of ZnO nanoparticles for azo dyes in wastewater treatment: A review. *Inorganic Chemistry Communications, 120,* 1–29. https://doi.org/10.1016/j.inoche.2020.108140

Yassumoto, L., Monezi, N. M., & Takashima, K. (2009). Descoloração de alguns azocorantes por processos de fotólise direta e H_2O_2/UV. *Semina: Ciências Exatas e Tecnológicas, 30*(2), 117–124. https://doi.org/10.5433/1679-0375.2009v30n2p117

Zhu, H., Jiang, R., Fu, Y., Guan, Y., Yao, J., Xiao, L., & Zeng, G. (2012). Effective photocatalytic decolorization of methyl orange utilizing TiO2/ZnO/chitosan nanocomposite films under simulated solar irradiation. *Desalination, 286,* 41–48. https://doi.org/10.1016/j.desal.2011.10.036

Semin., Ciênc. Exatas Tecnol. 2024, v.45: e49498

13